Direct Correlation between Interfacial Width and Adhesion in Glassy Polymers

Ralf Schnell and Manfred Stamm*

Max-Planck-Institut für Polymerforschung, Postfach 3148, 55021 Mainz, Germany

Costantino Creton*

Laboratoire de Physico-chimie Structurale et Macromoléculaire, ESPCI, 10 rue Vauquelin, 75231 Paris Cedex 05, France

Received July 10, 1997; Revised Manuscript Received November 24, 1997

ABSTRACT: The correlation between interfacial width and adhesion, as expressed by the fracture toughness of the interface, in glassy polymers is investigated. The interfacial width is measured accurately by neutron reflectivity, and the fracture toughness of the interfaces is determined from a double cantilever beam test. Two experimental situations are considered: the case of an interface between two immiscible polymers, polystyrene (PS) and poly(*p*-methylstyrene) (PpMS), and the case of a PS−PS interface, where the interfacial width and the fracture toughness are measured for different interdiffusion times. In both cases, a direct correlation between the fracture toughness and the interfacial width is found. After an initial rapid increase in toughness due presumably to chain-end diffusion, most of the subsequent increase in toughness occurs over a relatively narrow range of interfacial widths between 9 and 12 nm. The fracture toughness stays constant with further interdiffusion. The results are consistent with respect to a model where formation of entanglements is the determining factor for the development of adhesive strength at the interface.

Introduction

The adhesion between polymers plays an important role in several polymer processing and application areas where blending, welding, or coextrusion is involved. To control these processes in detail, it is useful to gain a detailed understanding of the interplay between the microscopic or the molecular structure of polymer interfaces and their macroscopic mechanical properties. In recent years, this has been a very active field, and several reviews exist on the subject.[1,2] It is useful to briefly outline here the main theoretical and experimental results describing the structure and strength of polymer interfaces.

At first, one should differentiate between two general types of interfaces: the case where the two polymers on either side of the interface are miscible, which are sometimes called symmetric interfaces, when the identical polymers are on both sides, and the asymmetric case where the two polymers on either side of the interface are immiscible. Note that this definition has nothing to do with the symmetry of the interfacial concentration profile, which is symmetric in both cases; only in the case of strong differences of T_g can the profile become asymmetric. In the first case, the problem is a kinetic one, where it is important to understand the dynamics of the diffusing chains across the plane of the interface, and the structure of the interface can be controlled with the annealing time and the molecular weight of the polymers.

In the second case, we are faced with a thermodynamic problem, where the detailed interactions between the segments of two immiscible polymers need to be understood. In this case, the equilibrium structure of the interface is not controlled with the annealing time but rather with the segment interaction parameter (χ) of the polymer blend (determined by the annealing temperature) and the molecular weight. Experiments of the kinetics of welding could be done with immiscible systems as well, although this is not our purpose in this paper. In many practical applications, of course, the situation is far from those ideal cases: systems may be partially miscible, the molecular weight distribution is broad, and the glass transition temperatures of components are different.

We will consider the thermodynamic case first: The structure of these interfaces has been mainly described with a mean-field approach aiming at the prediction (in a one-dimensional picture) of the monomer volume fraction normal to the plane of the interface.[3] The width of the tanh-shaped interface between incompatible polymers, for different molecular weights and temperatures, can be predicted if the Flory−Huggins interaction parameter (χ) and the Kuhn segment length (b) are known:[3]

$$a_i = a_{i,N=\infty}\frac{1}{\sqrt{1 - 2\ln 2\left(\frac{1}{\chi_{AB}N_A} + \frac{1}{\chi_{AB}N_B}\right)}} \qquad (1)$$

where $a_{i,N} = \infty$ is the theoretical interfacial width for polymers in the limit of infinite degrees of polymerization

$$a_{i,N=\infty} = \frac{2b}{\sqrt{\chi_{AB}\cdot c}} \qquad (2)$$

In the limit $a_i \ll R_g$ the prefactor $c = 6$ is given by Helfand and Tagami,[4] while the prefactor $c = 9$ is given in the limit $a_i \gg R_g$.[5] This theory, which describes interfaces between strongly segregated polymers at

* Authors to whom correspondence should be addressed.

S0024-9297(97)01020-6 CCC: $15.00
Published on Web 03/13/1998

thermodynamic equilibrium, was confirmed by several neutron reflectivity experiments (see, e.g., refs 6 and 7).

While the measurement of the interfacial width in immiscible polymer systems has attracted much attention, the corresponding measurements of the mechanical properties have been more difficult to perform. The main reason for this is that the fracture toughness in an adhesion experiment depends not only on the structure of the interface but also on the bulk properties of both polymers as well as on the experimental geometry, making it very difficult to compare the results obtained on different systems and by different groups. Ideally one can at least reduce the variables by working on the same polymer pair but with a variety of interfacial widths. However, only few polymer pairs exhibit the necessary variation in χ over an accessible range of temperatures. The choice of polystyrene (PS) and poly(*p*-methylstyrene) (PpMS) in the present work obeys that requirement.

For the case of symmetric polymer−polymer interfaces, on the other hand, the width of the interface evolves with time and the thermodynamic problem becomes a kinetic one involving the mechanisms of polymer interdiffusion. The most widely accepted model for the kinetics of interdiffusion in melts of chains with sufficiently high molecular weight is the reptation model, originally proposed by de Gennes[8] and further developed by Doi and Edwards.[9] This model has later also been applied to the interdiffusion of chains at an interface. It is assumed that, depending on the characteristic diffusion time or distance, the entangled polymer chains move mainly along their contour length (reptation tube). Motions in other directions are limited by entanglements with other chains. Because of this restriction, several different mechanisms of segmental diffusion are expected before the free Fickian diffusion can take place. At the early stages of diffusion time (t < entanglement time τ_e), where the average displacements of the chain segments $<r^2>^{1/2}$ are smaller than the diameter of the tube, the motion of chain segments is not yet influenced by entanglements with other chains. At diffusion times above τ_e, the motion in a direction perpendicular to the virtual tube becomes restricted by entanglements. The single-chain segments move along the virtual tube axis, which results in a $<r^2>^{1/2} \sim t^{1/8}$ law. Later, at the Rouse time (τ_R), correlated motions of the whole chain along the contour of the tube take place and $<r^2>^{1/2} \sim t^{1/4}$. At the reptation time (τ_{Rep}), the initial interface has disappeared and normal Fickian diffusion is observed: $\langle r^2\rangle^{1/2} \sim t^{1/2}$.

This model is qualitatively consistent with neutron reflectivity measurements.[10−13] Neutron reflectivity results during interdiffusion show a jump of the interfacial width after an initial annealing above T_g.[11,13−15] Within the reptation model, this might be identified with the Rouse-type motion of the chain segments within the tube, knowing that, in these investigations, τ_e was shorter than the shortest annealing times. Other possibilities have been discussed.[13,15] After this initial jump of a_i, the interfacial width is expected to be proportional to $t^{1/8}$ up to the τ_R. The exact time dependence in this regime was difficult to extract from experiments. But in this time regime, no strong increase of the interfacial width was observed experimentally. At annealing times above τ_R, the observed interfacial broadening corresponds reasonably well with the predicted $t^{1/4}$ and later with the $t^{1/2}$ behavior. It was often assumed that enrichment of chain ends was a possible reason for the differences in the first time regimes.[11,13] Recent experiments with end- and center-labeled PS chains have shown that the chain-end concentration is initially uniform for films prepared by spin-casting and that chain ends diffuse indeed much faster than the central segments of the chain.[16]

As opposed to the case of asymmetric interfaces, the testing of the mechanical strength of the symmetric interfaces is much less problematic, and several detailed studies are reported in the literature.[17−19] In these experiments, two sheets of the same polymer, which were either previously fractured (crack healing) or simply polished (welding), are put into close contact under mild pressure at temperatures above T_g for different annealing times. After quenching to room temperature, the interdiffusion process is frozen in and the fracture toughness between the two polymer sheets can be measured. It has been a tempting approach for many authors to directly correlate the predicted interfacial structure with the mechanical strength of the interface in order to compare the predictions of the reptation model for the interdiffusion distance with the macroscopic fracture toughness of the interface. An increase of the fracture energy (G_c) with $t^{1/2}$ was observed for different kinds of polymers. In early papers,[18] this behavior was interpreted qualitatively as being in good agreement with an increase in adhesion with time from chain interdiffusion as opposed to an increase of adhesion controlled by the wetting of the two surfaces. More recent papers interpret these results in light of the reptation theory, arguing that a $G_c \sim t^{1/2}$ dependence is characteristic of the reptation in a tube and should occur between τ_R and τ_d. Both interpretations rely on an assumed dependence between G_c and the interfacial width: in the first case, G_c was assumed to be proportional to a_i and in the second case to a_i^2. However, none of these approaches considered another important aspect of the interpretation of fracture toughness experiments on glassy polymers, namely, the relationship between the measured G_c and the micromechanisms of plastic deformation at the interface which are responsible for the energy dissipation. Recent investigations on the reinforcement of polymer interfaces with block copolymers have demonstrated that a necessary condition for a high adhesion is the formation of a plastic zone ahead of the propagating crack. Such a plastic zone can be formed if the stress that can be sustained by the interface is higher than the yield stress of at least one of the bulk materials on either side of the interface. Once formed, this plastic zone will then fail through a molecular event which can be either chain scission or chain pullout.

A recent model by Brown[20] has proposed a mechanism by which the maximum width of this plastic zone, and therefore the fracture toughness of the interface, is controlled by the areal density of strands crossing the plane of the interface. In his model, the molecular event responsible for the plastic zone failure is exclusively chain scission so that the fracture toughness is predicted to be molecular weight independent. In this regime (valid for high molecular weight polymers), G_c is predicted to scale with Σ^2, where Σ is the areal density of load-bearing strands crossing the plane of the interface

Table 1. Characteristics of Polymer Samples

polymer	M_w	M_w/M_n
polystyrene		
PS139	139.4	1.04
PS310	309.6	1.03
PS862	861.7	1.10
PS1.25 M	1250.7	1.11
PS(D)110	110	1.06
PS(D)714	714.3	1.04
poly(*p*-methylstyrene)		
PpMS131	131	1.05
PpMS157	157.1	1.06
PpMS570	569.6	1.14
PpMS613	613.1	1.11

(a value which is dependent only on M_e for bulk polymers).

In the case of reinforcement by block copolymers, the degree of entanglements between the block copolymer and the homopolymers is equally important as the areal density to achieve a high adhesion. In adhesion experiments on polystyrene−poly(2 -vinylpyridine) interfaces reinforced with corresponding block copolymers, the fracture toughness did not become independent of the molecular weight of the blocks until at least 5−6 times the average molecular weight between entanglements (M_e) was reached.[21] This result is in agreement also with fracture toughness experiments on pure PS,[2] showing that G_c only becomes molecular weight independent above $10-12M_e$.

In the case of reinforcement by block copolymers, usually the bare interface is very thin and allows very little interpenetration between the homopolymers, resulting therefore in a very low or negligible adhesion. In this case, it becomes possible to control independently the areal density of strands crossing the interface (only the block copolymer chains have to be taken into account, and one can assume a single crossing per chain) and their degree of entanglement with the homopolymer chains (controlled only by the molecular weight of the block if the homopolymer is long enough). On the contrary, for interfaces between weakly immiscible polymers, the interpenetration between the chains of the two homopolymers becomes significant and the areal density of strands (Σ) and their effectiveness (entangled length) can no longer be controlled independently. Both parameters are contained in a single experimentally accessible quantity, the interfacial width. None of the published studies has actually measured, however, the interfacial widths directly on the systems tested for fracture toughness. It is the goal of this paper to directly correlate the interfacial width obtained from neutron reflectivity measurements with the fracture toughness measurements of the same interfaces, utilizing essentially identical polymer materials in both cases.

Experimental Section

Materials. The polymers were obtained by anionic polymerization (Max-Planck-Institut für Polymerforschung) and have been characterized by gel permeation chromatography using PS standards. The relevant characteristics are listed in Table 1.

Fracture Toughness Tests. For asymmetric interfaces, PS and PpMS were separately compression molded at 160 °C into sheets (5 cm × 4 cm) with respective thicknesses of 2 and 3 mm. To obtain the sandwich samples, the PpMS and PS sheets were joined together in one mold and annealed at variable temperatures under slight pressure to obtain contact between the sheets. To ensure that the annealing time was long enough to reach equilibrium, comparable samples were annealed for different times. Samples were quenched to room temperature by putting the hot mold between two thick metal plates. These sandwich samples were then cut into 0.8-cm × 5-cm strips. For the symmetric interface tests, the PS sheets were prepared in a similar way except that they had an identical thickness of 2 mm. The annealing time for the sandwich samples was varied between 5 and 95 h and the annealing temperature was varied between 125 and 180 °C in order to obtain a distribution of interfacial widths.

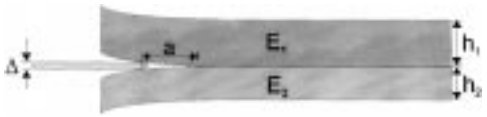

Figure 1. Schematic drawing of the ADCB test geometry and the important parameters.

The fracture toughness measurements between PS and PpMS were done using an asymmetric double cantilever beam (ADCB) as shown in Figure 1. If the thickness of both beams is the same, a crack propagating at an interface between these two polymers, which have different elastic constants, will not propagate in the pure opening mode (mode I) but in an opening and shear mode (mixed I and II mode), and this can result in the formation of small crazes at an angle from the interface. These small crazes result then in an increase of the apparent G_c. For very strong interfaces, the main crack may even deviate from the interface and go into the bulk material, making the measurement impossible. In these cases, an asymmetric geometry is necessary. As described by others,[22,23] the optimum sample geometry is usually at slightly negative values of the phase angle, ψ ($\tan\psi$ is defined as the ratio of the mode II over mode I stress intensity factors (k_{II}/k_I)). In this work, the optimum phase angle was determined empirically by varying the ratios of PS to PpMS thicknesses to minimize G_c.

Based on these observations, a sample geometry of 3-mm PpMS and 2-mm PS was chosen for the fracture toughness tests. Other ratios of thicknesses did cause the crack to leave the interface and to kink either into the PS or into the PpMS bulk phase. While we cannot exclude a slight overestimation of the absolute values for G_c, the measured values obtained with this method appeared to be sensitive to the structure of the interface.

To help the interpretation of experimental data, we also measured the crazing stresses and elastic moduli of both polymers by a three-point bending test as described by Creton et al.[21] They were determined to be 48 ± 5MPa for the crazing stress and 2.4 ± 0.2GPa for the elastic tensile modulus for PS (M_w = 1250 kg/mol) and 31 ± 5MPa and 2.1 ± 0.2GPa for PpMS (M_w = 570 kg/mol). As PpMS has a lower crazing stress and a lower elastic modulus, the PpMS side should be the preferred location for the plastic zone and should therefore be made thicker than the PS side to have a negative phase angle consistent with our experimental findings. For the welding experiments between two polystyrene sheets, there is no mixed mode problem and a symmetric geometry was chosen.

To determine the fracture toughness of polymer−polymer interfaces, a razor blade was inserted and pushed into the interface at a constant speed of 5 μm/s. The dependence of the fracture toughness on crack velocity was investigated in the range between 1 and 150 μm/s. As no significant dependence was observed, we assumed that the measured energy release rate at 5 μm/s is equal to G_c, the critical energy release rate at zero velocity. The resulting crack length was measured in situ using a video camera. To estimate G_c from the crack length a, we used the equation proposed by Kanninen,[24] who empirically takes into account the finite elasticity of the material ahead of the crack tip. This equation has been shown to give reliable results for polymer interfaces:[25]

$$G_c = \frac{3\Delta^2}{8a^4}\frac{E_1 h_1^3 E_2 h_2^3}{E_1 h_1^3 \alpha_2^2 + E_2 h_2^3 \alpha_1^2} \qquad (3)$$

the parameters h, a, and Δ are as explained in Figure 1. E_i is the Young modulus and α_i the respective correction factor for material i:

$$\alpha_i = \frac{(1 + 1.92h_i/a) + (1 + 1.22(h_i/a)^2) + (1 + 0.39(h_i/a)^3)}{1 + 0.64h_i/a}$$

Neutron Reflectivity Experiments. Thin polymer films (80−100 nm) were prepared by spin-coating a solution of the respective polymers in toluene onto silicon or float glass substrates. The obtained films were characterized by phase interference microscopy and X-ray reflectometry in terms of roughness and thickness. For the preparation of the double layers, one film was floated off the substrate onto a deionized water surface and picked up by a second film which was still on a substrate. After drying several days under vacuum at ambient temperature, the double-layer sample was investigated again with interference microscopy and X-ray reflectometry. After the precharacterization of the samples, neutron reflectivity experiments were performed on the neutron reflectometer TOREMA II at GKSS in Geesthacht, Germany. A fixed wavelength of 4.3 nm (graphite monochromator) and a variable incident beam were employed. A position-sensitive BF_3 detector was used for the investigations.

Neutron reflectivity allows us in a nondestructive way to determine interfacial widths (a_i) in the range between 2 and 30 nm with a resolution better than 0.5 nm. This method is sensitive to gradients of the refractive index (n)

$$n = 1 - \frac{\lambda^2}{2\pi} N_b \qquad (4)$$

where λ is the wavelength of the neutron beam and N_b the scattering length density of the polymer. The absorption is neglected in this formula.

Due to the big difference in scattering lengths between hydrogen and deuterium, it is possible to obtain sufficient contrast between the layers by using one deuterated film. The reflectivity data were analyzed with a model-dependent fitting procedure based on a matrix algorithm described by Lekner.[26] In agreement with mean-field theory for a concentration-independent χ parameter, we used a tanh-shaped interfacial profile to describe the volume fraction (ϕ) profile for the simulation of the reflectivity curves:

$$\phi(z) = 1/2\left[(\phi_1^B + \phi_2^B) + (\phi_1^B - \phi_2^B)\tanh\left(\frac{2(z - z_0)}{a_i}\right)\right] \qquad (5)$$

where z_0 is the center of the interface. The neutron reflectivity experiment is not very sensitive to the exact shape of the interface profile. Alternatively to the hyperbolic tangent function, it would be equally possible to simulate the interfacial profile by an error function. To simplify the comparison between differently defined interfacial widths, the correlation to the a_i used here should be given. The interfacial width of an error function is usually characterized by the variance (σ), where $(2\pi)^{1/2}\sigma$ equals a_i. A second definition of the interfacial width (α_i') is sometimes used in the literature, where the factor 2 in the argument of the tanh function in eq 5 is omitted: $a_i/2 = \alpha_i'$.

For the neutron reflectivity experiments, one deuterated film is always used, while for the fracture toughness tests, only protonated materials are employed.

Results

Determination of the Interfacial Width by Neutron Reflectivity, PS/PpMS. The width of the interface between PS and PpMS was investigated with neutron reflectivity for varying molecular weights and annealing temperatures. Samples have been annealed for long times until equilibrium is achieved. In Figure 2, the reflectivity curves (dots) of a PpMS(H) 131 kg/mol−PS(D) 714 kg/mol bilayer sample on float glass after annealing at different temperatures is shown. The upper curve represents the as-made sample. The Kiessig fringes are caused mostly by the deuterated layer. This is evidence for a sharp interface between the polymers. At increasing annealing temperatures, the interfaces broaden, as one can see indirectly in the successive changes of the reflectivity curves beginning at high k values. The air−polymer and polymer−substrate interfaces become more and more important for the reflectivity curve as the polymer−polymer interface loses contrast.

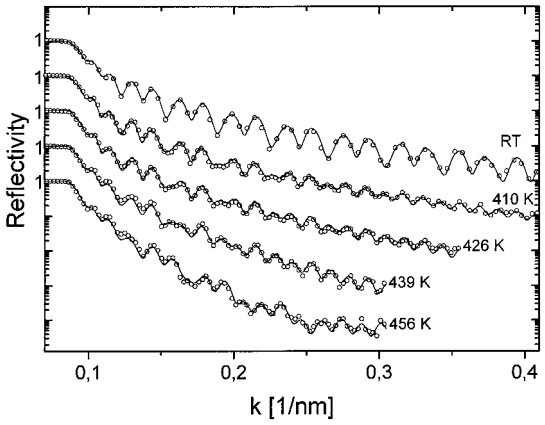

Figure 2. Neutron reflectivity data vs momentum transfer k of PS 714k/PpMS 131k bilayer samples after annealing at different temperatures. The reflectivity curves have been offset vertically for clarity. The solid lines represent the respective calculated reflectivity profile.

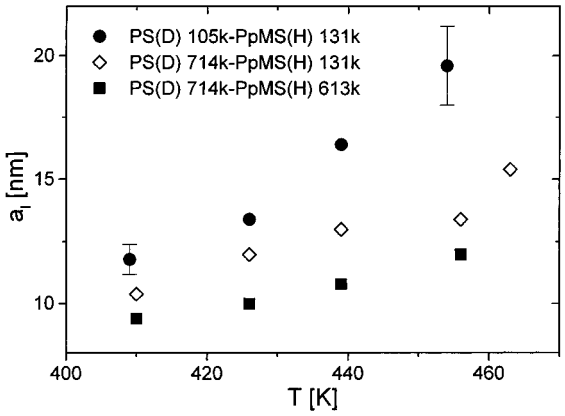

Figure 3. Fitted widths of the interfaces between the PS and PpMS layers as a function of annealing temperature.

The quantitative values of the interfacial width were determined by simulating the experimental data with a model-dependent fitting procedure assuming a tanh-shaped interface profile as described in eq 5. The good agreement between experimental data (dots) and simulation (solid lines) can be seen in Figure 2. The respective interfacial widths are shown in Figure 3, where values for additional molecular weights are also given.

By utilizing eq 1, one can calculate χ and the Kuhn segment length (b) from the interfacial width:

$$\chi = \frac{4b^2}{ca_i^2} + \left(\frac{2}{N_1} + \frac{2}{N_2}\right)\ln 2 \qquad (6)$$

As the interfacial widths of the samples with high molecular weights are clearly smaller than R_g, we used

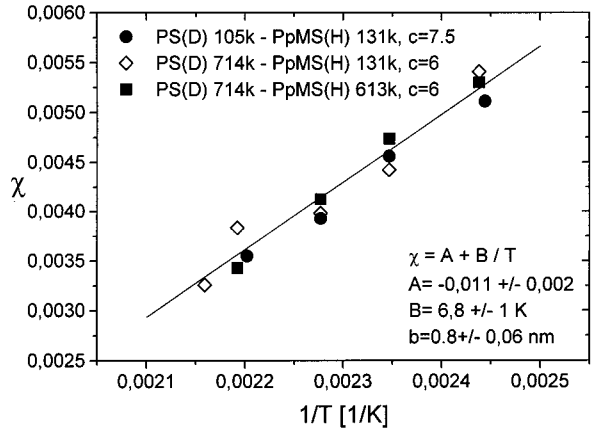

Figure 4. On the basis of a mean-field-theory by Broseta et al.,[3] calculated interaction parameters vs the reciprocal annealing temperature. Using the ansatz $\chi = A + B/T$, b was chosen in such a way that the data of different molecular weights fit in one linear master curve.

$c = 6$ to calculate the χ parameter. In the PpMS(H) 131 kg/mol−PS(D) 105 kg/mol sample, on the other hand, the interfacial width is of the order of R_g, and we chose $c = 7.5$, a value between 6 and 9. Using the ansatz $\chi = A + B/T$, b was chosen in such a way that the data of the different molecular weights fit a linear master curve (Figure 4). The resulting mean value of $b = 0.80 \pm 06$ nm is higher than the SANS value of 0.695 nm for pure PS[28] but in good agreement with the value found for PS−PpMS blends.[29] In Figure 4, the χ parameters are plotted vs the inverse temperature and can be described by $\chi(T) = -0.011 + 6.8/T$, where T is expressed in K.

As these χ parameters are in good agreement with SANS investigations of the same system,[29] one can conclude that lateral concentration fluctuations at the interface do not play an important role in the determined interfacial width. Following the arguments given by Semenov,[30] who discusses the influence of capillary waves from a theoretical viewpoint, this result, is not surprising for the investigated polymers. Shull et al.,[31] on the other hand, reported the influence of interface fluctuations on the interfacial width between PS and PMMA. In this more incompatible blend ($\chi = 0.04$), the mean-square displacement of the interface from its average position $[<(\Delta z)^2>]^{1/2}$ was estimated to be broader than $a_i/(2\pi)^{1/2}$. Therefore, the effective interfacial width can be expected to be dominated by lateral fluctuations for strongly incompatible polymers. As $[<(\Delta z)^2>]$ is expected to be proportional to $1/\chi^{1/2}$, the fluctuation contribution $[<(\Delta z)^2>]^{1/2}$ should be higher in the case of the less incompatible PS/PpMS interfaces. But, on the other hand, with decreasing χ a_i as described in eq 1 is growing faster than $[<(\Delta z)^2>]^{1/2}$. Therefore, in the investigated PS/PpMS samples, $a_i/(2\pi)^{1/2}$ is much larger than $[<(\Delta z)^2>]^{1/2}$ and the effect of interface fluctuations on the effective interfacial width turns out to be quite small after quadratic convolution. For a typical PS/PpMS interfacial width with $a_i = 10$ nm, the contribution of the lateral fluctuations as described by Semenov is estimated to increase the interfacial width by approximately 2 nm.

Determination of the Fracture Toughness: PS/PpMS. The fracture toughness of PS/PpMS bilayer samples is given in Figure 5 for different annealing temperatures and varying molecular weights. Except for the lowest molecular weight pair, the data show an increase of G_c with the annealing temperature and a decrease with increasing molecular weight in agreement with an increase in the interfacial width with increasing temperature and decreasing molecular weight.

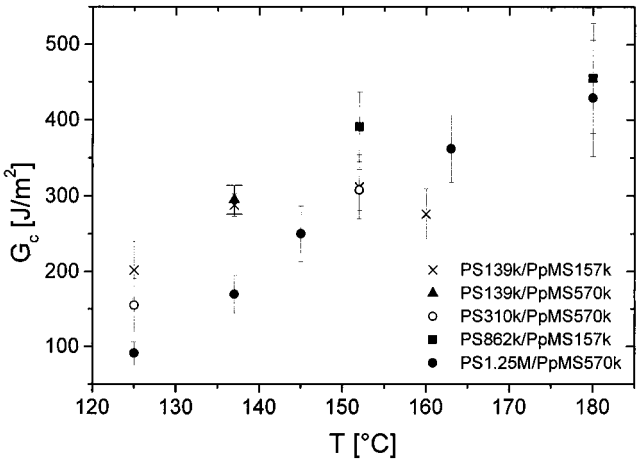

Figure 5. Plot of the strain energy release rate (G_c) of PS/PpMS samples with different molecular weights vs their annealing temperatures.

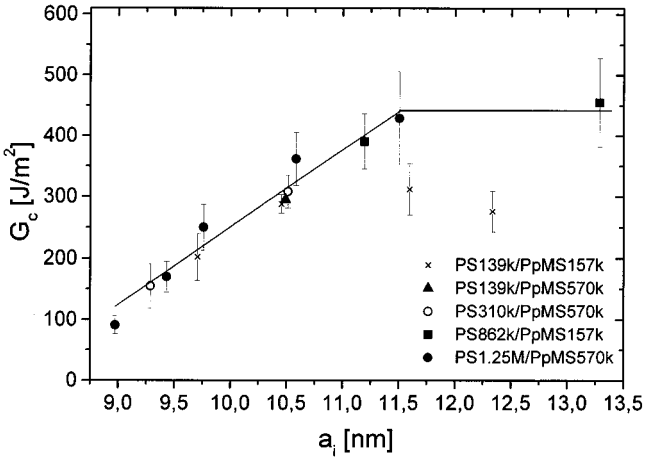

Figure 6. Adhesion energy (G_c) of different samples of PS/PpMS plotted as a function of the interfacial width (a_i). The solid line is drawn as a guide to the eye.

Given that identically synthesized polymers were used for the NR measurements and the fracture toughness investigations, we can directly relate the interfacial width of a particular polymer pair to its fracture toughness. The respective values for the interfacial widths were extrapolated from our neutron reflectivity data using eq 6 and the empirically determined values for b and χ. It must be emphasized that ADCB measurements require a different sample preparation compared to the neutron reflectivity investigations, but the geometry remains planar, and the interfaces are at thermodynamic equilibrium. We cannot, however, exclude completely that sample geometry may also have an effect.[32]

As shown in Figure 6, at interfacial widths below 11 nm, the fracture toughness seems to be well correlated with the width of the interface. The measured points obtained with different molecular weight combinations and at different temperatures fall on a single curve. It is interesting to note that Foster and Wool did not find such a correlation for PS−PMMA interfaces. In their case, the variation in interfacial width with temperature was negligible,[2] and they therefore could not cover such a wide range of a_i values.

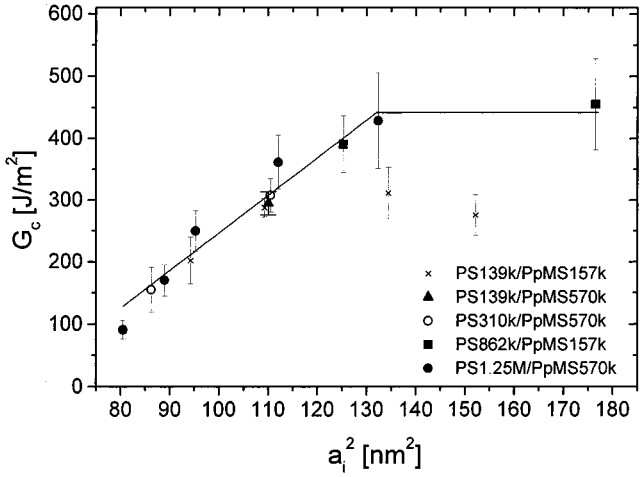

Figure 7. Adhesion energy (G_c) plotted vs the square of the interfacial width (a_i^2) (same data as is Figure 6). The solid line is a guide to the eye.

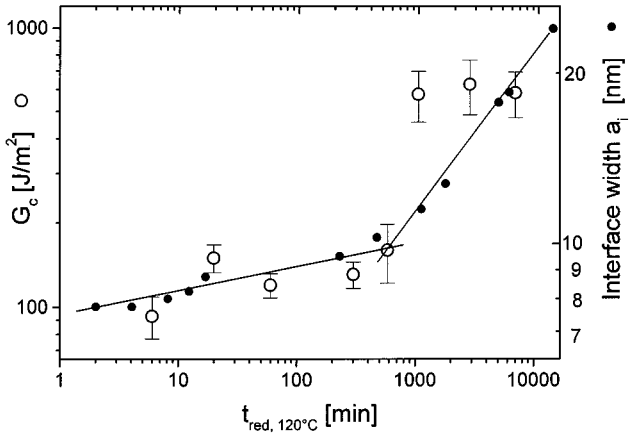

Figure 8. Double logarithmic plot of the adhesion energy (G_c) of PS/PS 862k vs the reduced annealing time ($t_{red,120}$). To compare theses data with respective interfacial widths, neutron reflectivity data of PS(D) 752k/PS(H) 660k bilayer samples by Stamm et al.[15] are included in the plot (see right *y* axis).

This shows that, for high molecular weight polymers (with $N \gg N_e$), the interfacial width proves to be the main parameter controlling the fracture toughness of the interface of the given pair of polymers. When the interfacial width was larger than 12 nm, the determination of G_c became difficult because the crack kinked easily away from the interface. This was taken as evidence that the measured values of the adhesion energy were already close to the bulk values. In this regime, no further increase of the fracture toughness was observed with interfacial width. One should note, however, that while this situation is true for high molecular weight polymers, the measured points for PS 139 kg/mol/PpMS 157 kg/mol do not reach the same level of fracture toughness as the samples with higher molecular weights.

Given the open question of the dependence of G_c on a_i, it was interesting to see whether our data correlated best with a_i or a_i^2. Due to the onset of plastic deformation mechanisms giving rise to a transition in G_c, one does not expect the data to extrapolate at $G_c = 0$ for a vanishing interfacial width, and it is best to plot our data vs a_i and a_i^2 as shown in Figures 6 and 7. In both cases, the data can be represented by an expression of the type $G_c = G_{c_0} + a_i^n$, where $n = 1$ or 2. However, due to the limited range of a_i and the large effect on G_c, we cannot distinguish, within the scatter of our data, which exponent would give a better fit.

Symmetric Interfaces: PS/PS. To study the kinetics of welding, we performed interdiffusion experiments between PS/PS samples with an identical molecular weight (862k). Since the interesting time range of interdiffusion covers several decades, the annealing was done at different temperatures and reduced to the reference temperature of 120 °C using the WLF equation for PS:[33]

$$\log a_T = -9.06(T - 120)/(69.8 + T - 120)$$

To obtain the reduced annealing time (t_{red}), the real annealing time (t) was divided by a_T. In Figure 8, the adhesion energy is plotted vs the reduced annealing time. For comparison with the corresponding interfacial widths, some NR results of PS(D) 752k/PS(H) 660k bilayer samples by Stamm et al.[15] are given on the same plot. Data have been scaled to each other by some arbitrary factor. The fast increase of the interfacial width after the first annealing above T_g as observed by NR can be indirectly confirmed by the welding experiment, where an adhesion energy of 93 ± 16 J/m^2 was measured already after $t_{red} = 6$ min. One should note, however, that the initial stages of polymer interdiffusion of thick samples, such as those necessary for toughness tests, are convoluted with the kinetics of wetting of the substrate. After this first jump, only a weak increase of the adhesion energy was determined up to $t_{red,120} = 585$ min. This seems to be in good agreement with the NR investigations, where only a slight increase of the interfacial widths was observed up to the Rouse time. Close to the Rouse time, a steep increase of the fracture toughness up to a constant value of approximately 600 J/m^2, very close to the bulk fracture toughness, was observed, implying a distinct change of fracture mechanism.

Discussion

Our results on PS/PpMS interfaces show within experimental errors that a_i can be used as a single parameter ("master curve") to characterize the adhesion of the interface provided that the molecular weights of the homopolymers are high enough.

The combined use of the two techniques, neutron reflectivity and fracture toughness measurements with the same materials, provides us with a unique correlation between interfacial width and corresponding adhesion. Choosing the system PS/PpMS has the advantage that, since the polymers are only weakly incompatible, a relatively wide range of interfacial widths can be investigated by varying the molecular weight of each component and the annealing temperature. From the plot of fracture toughness vs interfacial width (Figure 6 or 7), one may distinguish two main regimes and suspect the existence of a third one:

(a) At intermediate values of a_i, G_c increases with increasing a_i, and the fracture toughness is relatively high and is controlled by the molecular failure mechanisms of a plastic zone formed ahead of the propagating crack. We will define it as regime ii.

(b) At high values of a_i, G_c has reached its bulk value and does not change with a_i any more. The main evidence for this regime is the fact that the crack kinked out of the interface on either the PS or the PpMS side of the interface for most of the fracture propagation

experiments in those conditions. This shows that we are indeed close to the bulk fracture toughness. However, because of this limitation, only in few cases were we able to obtain valid experimental points in this regime, which we will define as regime iii.

(c) At low values of a_i, one can suspect the existence of a third regime. The reason for this becomes evident if one extrapolates the data in Figure 6 to small interfacial widths: the fracture toughness would extrapolate at zero for $a_i = 8$ nm. Since this is not physical, one can postulate the existence of a third regime, defined as regime i, where the fracture toughness increases less steeply with increasing interfacial width, or a discontinuous jump in toughness G_c for a critical value of a_i.

The transition from regime i to ii is probably connected with a transition in the crack propagation mechanism, i.e., the development of the plastic zone as was observed in interfaces reinforced with block copolymers.[21]

On a more microscopic level, we can assume that regime ii is dominated by the formation of entanglements on both sides of the interface, while regime i is dominated by chain pullouts.

The importance of a_i in regime ii is essentially consistent with the hypothesis that Σ approaches very quickly its bulk value and the relevant parameter is then only the interpenetration length. This hypothesis, also postulated by Brown, is reasonable if one assumes that chain ends diffuse very quickly across the interface. In the framework of Brown's model for craze failure, one can postulate some molecular mechanisms of failure. If crazing is the main energy-dissipating mechanism, the measured fracture toughness is directly proportional to the maximum width of a craze ahead of a crack. This maximum width is in turn proportional to the square of the areal density of connecting chains and to the square of the force (f) to break (or pullout) a molecular strand. If one first starts from the experimental result that G_c increases linearly with a_i and assumes that Σ remains constant, then this leads to a f proportional to $s^{1/4}$, where s is the contour length of the interpenetrated part of the chain. On the other hand, a dependence of G_c with a_i^2 would imply a pullout force proportional to $s^{1/2}$. In either case, the dependence of the pullout force on contour length would then be much weaker than in the straight pullout case investigated by Washiyama et al.[37] where f turns out to be proportional to s. As pointed out by Brown,[1] this is not really surprising, as the chains are probably disentangled as bundles from the craze fibril rather than pulled out individually. In addition, the assumptions of constant Σ may not be true and the effects of chain ends, distorted chain conformation, or orientation as observed in the model calculations[38] are not taken into account. The functional dependence of f or G_c on a_i is therefore difficult to predict, since neither the chain conformation at the interface nor the pullout mechanism is presently known in detail.

Another important point obtained from our results is that the adhesion becomes independent of the interfacial width for $a_i > 11$ nm. This value corresponds roughly to the average distance between mechanically effective entanglement points in PS (9.3 nm), [the average distance between entanglement points can be evaluated using the relation $d^2 = C_\infty {l_0}^2 M_e m_0^{-1}$, where $C_\infty = 10.5$ for PS (Xu, Z.; Hadjichristidis, N.; Fetters, L. J.; Mays, J. W. *Adv. Polym. Sci.* **1995**, *120*, 1−50), M_e is the average molecular weight between entanglement points (18 000 for PS (Onogi, S.; Masuda, T.; Kitagawa, K. *Macromolecules* **1970**, *3*, 109−116)), m_0 is the molar mass per backbone bond (52 for PS), and l_0 is the length of a C−C bond (1.54 Å)] but is much shorter than the radius of gyration of the polymers (for example, 21.3 nm for 570 PS) which could imply that the polymer chain needs only to interpenetrate roughly by an entanglement distance to provide an optimum adhesion. When lower molecular weight polymers are used, as in the case of PS/PpMS 139k/157k, G_c saturates for a slightly lower value of $a_i = 10.5$ nm (which now corresponds more closely to an R_g of ∼10.4 nm for 139k PS, consistent with an argument saying that, for lower molecular weight polymers, the bulk strength is recovered when the interpenetration distance becomes comparable to R_g) and, more importantly, the fracture toughness decreases by approximately 25% relative to the high molecular weight value. This result can be understood by a loss in bulk fracture toughness of both adherends. Wool has shown that the bulk PS fracture toughness only becomes independent of molecular weight when $M > 10-12\ M_e$.[19]

Turning to the PS welding results, a surprising feature of our data is that the fracture toughness of PS increases only slightly with time until approximately 500 min of annealing at 120 °C, and then discontinuously jumps to a value close to the bulk fracture toughness, which does not change anymore with annealing time. This is in apparent contradiction with most other results where G_c increases with $t^{1/2}$.

To understand this apparent discrepancy, one must examine critically two general hypotheses which are often assumed implicitly:

(1) For a given interdiffusing polymer of degree of polymerization $N > 10-12N_e$ and for times $t < \tau_d$, there is a unique relationship (independent of molecular weight) between the interfacial width at t and the fracture toughness of the resulting interface.

(2) For a given N, the dependence of the fracture toughness on the interdiffusion distance can be described by a single power law exponent over a wide range of diffusion distances.

Let us discuss the first hypothesis: In the limiting case of low molecular weights, the maximum fracture toughness of the interface is achieved when the chains are interpenetrated over a certain characteristic distance a_i* related to their size. On the other hand, at the value of molecular weight of $10-12M_e$ where bulk toughness becomes molecular weight independent, there must be a crossover to a regime where a_i* becomes molecular weight independent and is related to the average distance between entanglements. Although we do not know precisely what the chain conformation will be at the interface, we can still propose a possible estimate for the high molecular weight limiting value of a_i*. From our results for PS/PpMS interfaces, there appears to be a difference in a_i* only for the lower molecular weight pair investigated (where a_i* decreases from 11 to 10.5 nm). The distance related to molecular size which is closer to 10.5 nm is the radius of gyration (10.5 nm for 139 PS).

Therefore, one can postulate the following mechanism:

For $M < 12M_e$, a_i* is given by

$$a_i^* = R_g = l_0(C_\infty M/6m_0)^{1/2} \quad (7)$$

However, for $M > 12M_e$, the interpenetration distance is independent of M and becomes related to M_e only:

$$a_i^* = l_0(12C_\infty M_e/6m_0)^{1/2} \quad (8)$$

In our case, the molecular weight of the interdiffusing PS is almost 50 times the entanglement molecular weight and we expect to be in the regime where a_I^* is molecular weight independent. The measured value of a_I^* is between 10.0 and 12.0 nm for our PS, which is reasonably consistent with a theoretical value as given by eq 8 of 13.1 nm.

Such a qualitative behavior has been also postulated by Wool,[2] who argued, however, that the maximum toughness for $M < 12M_e$ was achieved when the interfacial width $a_i > (2\pi)^{1/2}\ 0.81R_g$. We believe that the use of R_g as a critical distance is more consistent with our experimental data but are well aware that a more definite conclusion would require further careful investigations on other systems and molecular weight pairs.

The only other case that we are aware of where interfacial width data and fracture data have been published is for PS 233 (interfacial width)[14] and PS 207 (fracture).[2] In this case, the fracture toughness had reached a maximum after around 400 min of annealing at 120 °C, and this would have given an a_i between 17.5 and 22.5 nm, which is much higher than the R_g for this polymer (∼12.5 nm). In this case, a different critical distance than R_g appears to be important. However, the apparent discrepancy between our result and this result could be due to the fact their interfacial data have not been corrected for initial roughness and molecular weights are significantly different. One must bear in mind that in these interdiffusion experiments, the initial chain conformation and the wetting kinetics in the early stages may considerably influence the kinetics, biasing therefore our interpretation.

Nevertheless, it is not obvious that the fracture toughness of the interface at a given interfacial width value (corresponding to different interdiffusion times t for different molecular weights) has to be the same and a more systematic investigation of the critical interfacial width a_I^* as a function of molecular weight of the interdiffusing polymers would be necessary to be more affirmative on the dependence of G_c on the interfacial width.

The second assumption that needs to be critically examined is that of the unique power law dependence of the fracture toughness as a function of time.

The hypothesis clearly does not hold for very short annealing times where wetting of the surface is convoluted with the very rapid interdiffusion of the chains over a distance comparable to the Doi−Edwards tube length. Interestingly, all fracture data obtained at very short times show at least a toughness of the order of 100 J/m^2. At longer annealing times, two types of behavior should be observed: For moderately high molecular weights, the increase in adhesion occurs for times of annealing which are between the Rouse time and the reptation time of the polymer. In this case, one expects to see a single power law dependence of G_c as a function of annealing time, corresponding to the progressive increase of the interfacial width which causes an increased craze stability. Experimentally many investigators have found $G_c \sim t^{1/2}$. On the other hand, for very high molecular weights, the increase in toughness occurs over two diffusion regimes: between τ_e and τ_R, where, experimentally, toughness increases very little with time, and between τ_R and τ_d, where one expects to see a $t^{1/2}$ dependence. For our PS data, the Rouse time is of the order of 150 min at $T = 120$ °C so that the slow increase in toughness at short annealing times may be due to the weak time dependence of the diffusion distance between τ_e and τ_R. Given the experimental uncertainty of the data, the observed discontinuous jump in G_c at approximately $t = 900$ min can then be interpreted as a transition to a short $t^{1/2}$ behavior followed immediately by a plateau, indicating a change in the molecular mechanisms responsible for the craze failure at the crack tip from chain pullout to chain scission.

A final important point deserves to be mentioned regarding the relationship between interfacial width and fracture toughness.

In these welding experiments between homopolymers, the measured interfacial width to obtain $G_c = 100$ J/m^2 is of the order of 7.0−8.0 nm, which is distinctly lower than the average length between entanglement points (9.3 nm for PS). Therefore, one must assume that in such an interdiffusion geometry, the chains can entangle reasonably well (enough to sustain a stress of the order of the crazing stress of PS) even over a short interpenetration distance. This case should be compared with the case of A/B block copolymers at the interface between A and B homopolymers. Mean-field simulations[34] have shown that, if the copolymer chains are not stretched, the width of the interface between a tethered chain (in this case the block) and the homopolymer is approximately $2R_g$. Fracture toughness experiments on interfaces between polystyrene and poly(2-vinylpyridine) (PVP) reinforced with PS−PVP block copolymers have shown that for a block homopolymer interfacial width of less than ∼7.0 nm, the fracture toughness is below 5 J/m^2. To obtain 100 J/m^2, the required interfacial width is approximately 15.0 nm![21] Therefore, the mechanical effectiveness of the entanglements must be very different in the two cases. This could be due to a different entanglement topology. Thus, a diblock copolymer at the interface of strongly incompatible homopolymers is believed to form a brushlike conformation. The copolymer is thus stretched perpendicular to the interface, which should result in less entanglements as compared to the isotropic melt. A completely stretched chain (ideal brush) would have no entanglements at all. Therefore, due to this stretching effect, the interface has to be wider to obtain the same number of entanglements as compared to the isotropic case. A homopolymer chain, on the other hand, will also not be isotropic at the interface[38] but would show the opposite effect on orientation in the plane of the interface (pancake conformation). This may even lead to a larger number of effective entanglements perpendicular to the interface as compared to the isotropic case. The differences in fracture toughness may reflect the different chain conformations at the interfaces for two cases connected with a different entanglement topography.

Conclusions

The goal of this paper was to investigate the validity of the generally accepted assumption that the measured fracture toughness between two glassy polymers is directly related to their interfacial width.

The salient results are the following:

(1) For the immiscible PS−PpMS pair, there is a unique relationship between the interfacial width and the fracture toughness provided that the molecular weights of both homopolymers are high enough to achieve mechanically effective entanglements.

(2) For the PS−PS interfaces, the G_c dependence on the annealing time qualitatively parallels that of the interfacial width until the latter reaches approximately 13.0 nm, at which point G_c reaches the bulk toughness and becomes independent of the interfacial width.

(3) For both cases, a very large increase in toughness (from 100 to approximately 500 J/m^2) occurs over a relatively small range of interfacial widths, between 9 and 11 nm. This increase is attributed to the onset of sufficient entanglements to raise the stability of the fibrils of an interfacial craze to the level of a craze occurring in the bulk homopolymer.

(4) From our experimental data, one can postulate a functional dependence of the type $G_c = G_{c_0} + a_i^n$ for the fracture toughness. Based on what is known about the fracture behavior of glassy polymers, G_{c_0} is the smallest measurable toughness where a stable plastic zone forms. Due to the limited range of accessible interfacial widths, our experimental results could be equally well fitted with an exponent $n = 1$ or 2.

(5) The interfacial width required to obtain bulk toughness is significantly lower in the case of an interface between two homopolymers than between a tethered chain (brush or block copolymer) and a homopolymer, implying therefore a different entanglement topology between the two experimental situations.

One should note also that, as pointed out by others,[35,36] the average molecular weight between entanglements should play a major role in the critical interfacial width and provide a way to test some of these ideas on the effect of entanglements by using polymers with different values of N_e.

Acknowledgment. This work was supported by DFG within Graduiertenkolleg “Chemie und Physik supramolekularer Systeme”. Neutron experiments were performed within a collaboration agreement between GKSS and MPI-P and the help of Dr. D. W. Schubert and C. Ruppel, which are greatly acknowledged. We are grateful to T. Wagner for the preparation of the polymers.

References and Notes

(1) Brown, H. R. *Ann. Rev. Mater. Sci.* **1991**, *21*, 463.
(2) Wool, R. P. *Polymer Interfaces*, 1st ed.; Hanser Verlag: München, 1995.
(3) Broseta, D.; Fredrickson, G. H.; Helfand, E.; Leibler, L. *Macromolecules* **1990**, *23*, 132.
(4) Helfand, E.; Tagami, Y. *J. Chem. Phys.* **1971**, *56*, 3592.
(5) Anastasiadis, S. H.; Gancarz, I.; Koberstein, J. T. *Macromolecules* **1988**, *21*, 2980.
(6) Schubert, D. W.; Abetz, V.; Stamm, M.; Hack, T.; Siol, W. *Macromolecules* **1995**, *28*, 2519.
(7) Guckenbiehl, B.; Stamm, M.; Springer, T. *Phys. B* **1994**, *198*, 127.
(8) de Gennes, P. G. *J. Chem. Phys.* **1971**, 572−579. de Gennes, P. G. *C. R. Acad. Sci. Paris, II* **1989**, *308*, 13.
(9) Doi, M.; Edwards, S. F. *The Theory of Polymer Dynamics*; Clarendon: Oxford, 1986.
(10) Felcher, G. P.; Karim, A.; Russell, T. P. *J. Non-Crystall. Solids* **1991**, *131−133*, 703.
(11) Kunz, K.; Stamm, M. *Macromolecules* **1996**, *29*, 2548.
(12) Reiter, G.; Steiner, U. *J. Phys. II* **1991**, *1*, 659.
(13) Stamm, M. In *Physics of Polymer Surfaces and Interfaces;* Sanchez, I. C., Ed.; Butterworth-Heinemann: Boston, 1992; p 163.
(14) Karim, A.; Mansour, A.; Felcher, G. P. *Phys. Rev. B* **1990**, *42*, 6846.
(15) Stamm, M.; Hüttenbach, S.; Reiter, G.; Springer, T. *Europhys. Lett.* **1991**, *14*, 451.
(16) Russell, T. P.; Deline, V. R.; Dozier, W. D.; Felcher, G. P.; Agrawal, G.; Wool, R. P.; Mays, J. W. *Nature* **1993**, *365*, 235. Agrawal, G.; Wool, R. P.; Dozier, W. D.; Felcher, G. P.; Zhou, J.; Pispas, S.; Mays, J. W.; Russell, T. P. *J. Polym. Sci., Polym. Phys.* **1996**, *34*, 2919.
(17) Kausch, H. H.; Tirrell, M. *Annu. Rev. Mater. Sci.* **1989**, *19*, 341.
(18) Jud, K.; Kausch, H. H. *Polym. Bull.* **1979**, *1*, 697.
(19) Wool, R. P.; Yuan, B.-L.; McGarel, O. J. *Polym. Eng. Sci., Mid-Oct.* **1989**, *29*, 1340.
(20) Brown, H. R. *Macromolecules* **1991**, *24*, 2752.
(21) Creton, C.; Kramer, E. J.; Hui, C.-Y.; Brown, H. R. *Macromolecules* **1992**, *25*, 3075.
(22) Xiao, F.; Hui, C.-Y.; Washiyama, J.; Kramer, E. J. *Macromolecules* **1994**, *27*, 4382.
(23) Brown, H. R. *J. Mat. Sci.* **1990**, *25*, 2791.
(24) Kanninen, M. F. *Int. J. Frac.* **1973**, *9*, 83.
(25) Boucher, E.; Folkers, J. P.; Hervet, H.; Léger, L.; Creton, C. *Macromolecules* **1996**, *29*, 774.
(26) Lekner, J. *Theory of Reflection*; Martinus Nijhoff: Dordrecht, 1987.
(27) Schubert, D. W.; Stamm, M. *Europhys. Lett.* **1996**, *35*, 419.
(28) Wignall, G. D.; Ballard, D. G. H.; Schelten, J. *Europ. Polym. J.* **1974**, *16*, 861.
(29) Jung, W. G.; Fischer, E. W. *Makromol. Chem., Macromol. Symp.* **1988**, *16*, 281.
(30) Semenov, A. N. *Macromolecules* **1993**, *26*, 6617.
(31) Shull, K.; Mayes, A. M.; Russell, T. P. *Macromolecules* **1993**, *26*, 3929.
(32) Kerle, T.; Klein, J.; Binder, K. *Phys. Rev. Lett.* **1996**, *77*, 1318.
(33) Tassin, J. F.; Monnerie, L.; Fetters, L. J. *Macromolecules* **1988**, *21*, 2404.
(34) Shull, K. R. *J. Chem. Phys.* **1991**, *94*, 5723.
(35) de Gennes, P. G. *C. R. Acad. Sci. Paris Sér. II* **1989**, 1401.
(36) Creton, C.; Brown, H. R.; Deline, V. R. *Macromolecules* **1994**, *27*, 1774.
(37) Washiyama, J.; Kramer, E. J.; Creton, C.; Hui, C. Y. *Macromolecules* **1994**, *27*, 2019.
(38) Müller, M.; Binder, K. *J. Chem. Soc., Faraday Discuss.* **1995**, *9*, 2369.

MA971020X